OPTIMIZATION OF SYNTHESIS OF SHAPE – STABILIZED PHASE CHANGE MATERIALS CONTAINING NaCl – NaBr – Na_2MoO_4 AND MESOPOROUS SILICA

Daniel LINCU [1], Simona IONIȚĂ [2], Oana Cătălina MOCIOIU [3], Raul-Augustin MITRAN [4], Cristian MATEI [5], Daniela BERGER [6]

Fossil fuels are a limited resource, as they formed over millions of years in the Earth's crust. Their use also has significant environmental impacts such as air and water pollution, greenhouse gas emissions and habitat destruction. Renewable energy sources must be developed as soon as possible. Solar energy is a renewable energy source, which can be harvested through concentrated solar power plant into a thermal energy storage system. Shape – stabilized phase change materials are suitable in such power plants as thermal energy storage (TES) batteries. In this study, obtaining of phase change material (PCM) composites based on NaCl–NaBr–Na_2MoO_4 eutectic and mesoporous silica (MS) is optimized. Several eutectic-MS compositions are obtained and characterized. The resulted materials are shape – stabilized, thermally stable up to 650 °C and have a total enthalpy in the range of 100 – 211 Jg^{-1}. PCM composites have a lower melting point than that of the salt eutectic suggesting the nanoconfinement of the eutectic into MS. Some samples exhibit a better thermal reliability and show more evidence of nanoconfinement effect. The obtained shape – stabilized PCMs could act as thermal batteries.

Keywords: Phase change materials, shape – stabilized composites, mesoporous silica, nanoconfinement effect, molten salts

[1] PhD student, Dept. of Inorganic Chemistry, Physical Chemistry and Electrochemistry, National University of Science and Technologies POLITEHNICA Bucharest, Romania and Res. Asst., "Ilie Murgulescu" Institute of Physical Chemistry, Romania e-mail: daniel.lincu1113a@gmail.com

[2] PhD student, Dept. of Inorganic Chemistry, Physical Chemistry and Electrochemistry, National University of Science and Technologies POLITEHNICA Bucharest, Romania and Res. Asst., "Ilie Murgulescu" Institute of Physical Chemistry, Romania e-mail: ionitasimona05@gmail.com

[3] Researcher, "Ilie Murgulescu" Institute of Physical Chemistry, Romania e-mail: oana.mocioiu@yahoo.com

[4] Researcher, "Ilie Murgulescu" Institute of Physical Chemistry, Romania e-mail: raul.mitran@gmail.com

[5] Prof., Dept. of Inorganic Chemistry, Physical Chemistry and Electrochemistry, , National University of Science and Technologies POLITEHNICA Bucharest, Romania e-mail: cristian.matei@upb.ro

[6] Prof., Dept. of Inorganic Chemistry, Physical Chemistry and Electrochemistry, National University of Science and Technologies POLITEHNICA Bucharest, Romania e-mail: daniela.berger@upb.ro

1. Introduction

Solar energy is a type of renewable energy, which is not yet fully exploited due to the competitiveness with generating energy from non-renewable resources [1]. This type of renewable energy has several advantages, such as being a clean and sustainable source that can reduce greenhouse gas emissions and dependence on fossil fuels. However, one of the primary challenges associated with the harnessing of solar energy is that it is intermittent and depends on environmental factors such as weather conditions. This makes it difficult to use as a primary source of energy without a reliable method of storing excess energy for use during periods when sunlight is not available. This is where the innovation of thermal batteries or Thermal Energy Storage technology (TES) comes into play.

A type of thermal energy storage system employs phase change materials (PCMs) that can undergo reversible phase change while absorbing or releasing large amounts of thermal energy as latent heat at a constant temperature. In addition, the sensible heat storage can also function as energy storage and the latent and sensible heat approaches can be combined [2, 3].

There are many types of chemical compounds that can be used as PCMs. Inorganic substances such as hydrated salts, molten salts, metals, and organic substances such as paraffins, fatty acids, polymers etc. [4].

One of the primary limitations of PCMs, especially in the case of molten salts, is the molar volume change during solid - liquid phase transition, which can lead to the deterioration of the storing tank, leakage, decreased thermal transfer and eventually to an inoperable installation [5]. Therefore, the molar volume change associated with solid-liquid phase transition is a major drawback of using PCMs in thermal energy storage applications.

To overcome this major drawback, two approaches can be employed: encapsulation [6, 7] and impregnation into a matrix [8]. The resulting composite materials are called shape - stabilized PCMs and they can maintain their macroscopic shape even when the heat storage medium is in molten state. The phase change material encapsulation determines shape stability by resulting in a solid barrier, while impregnation achieves it through increased viscosity and capillary forces between the solid matrix and melted PCM. The impregnation approach uses less matrix material and therefore has a higher heat storage capacity, but there is a risk of PCM loss due to evaporation.

Mesoporous silica is widely used as matrix in shape – stabilized PCMs where organic compounds such as paraffins [9, 10], fatty acids [11-13], polymers-PEG [14, 15] and inorganics like hydrated salts [16, 17], molten salts [18, 19] and even metals [8] are used as the active heat storage phase.

Mesoporous silica (MS) is a matrix with a great potential for high-temperature applications when molten salts are used as active heat storage phase. MS has a high porosity, with specific surface area values that can exceed 900 m^2g^-

[1] and a total pore volume ranging from 0.5 and 3.5 cm^3g^{-1} [20-22]. MS can be easily obtained through sol–gel method with textural and morphological properties that can be tailored by adjusting the synthesis parameters [23]. Furthermore, MS is a non – toxic, chemically, and thermally stable up to 900 °C material [24], which makes it suitable as a matrix for shape – stabilized composite materials.

High-temperature phase change materials can be employed in concentrated solar power (CSP) technology [25, 26]. For this application, the ternary eutectic mixture consisting in 5% NaCl, 40% NaBr and 55% (mol) Na_2MoO_4 is used as previously reported [27], owing to its high melting point of ~524 °C and large enthalpy value of 215 Jg^{-1}. The optimum matrix for the ternary eutectic was identified as mesocellular foam silica (MCF) in a previous study [27]. For the first time, the effect of PCM loading is reported. MCF-based high temperature PCMs with 70%, 80%, 85% and 92.5% wt. eutectic content were synthesized through an optimized impregnation method. Thermal properties such as shape stability, heat storage capacity, thermal stability and reliability were investigated.

2. Experimental

2.1. Materials and reagents

Tetraethyl orthosilicate (TEOS), 1,3,5-trimethylbenzene (TMB), Pluronic P123 (poly(ethylene glycol)$_{20}$-block-poly(propylene glycol)$_{70}$-block-poly(ethylene glycol)$_{20}$, average molar weight 5800), ethanol, and 37% hydrochloric acid (HCl 37%), NaCl, NaBr, $Na_2MoO_4{\cdot}2H_2O$, NH_4F, were purchased from Sigma Aldrich and used as received. Ultrapure water was used for all syntheses. All salts were reagent grade.

2.2. Synthesis of mesocellular foam-type silica

12.76 g Pluronic P123 were dissolved in 207.35 mL ultrapure H_2O and 31.85 mL concentrated HCl at room temperature. Then, 18.46 mL of TMB was added and the reaction mixture was stirred for 2 h at 40 °C. Next, 29.35 mL of TEOS was added to the solution and stirred for 5 min. The reaction mixture was aged at 40 °C for 24 h under static conditions. Later 142.6 mg of NH_4F were added and the resulting mixture was transferred to a Teflon-lined autoclave for 24 h solvothermal treatment at 140 °C. The resulting particles were filtered off, washed with ethanol and water, dried and calcined at 550 °C for 5h [8].

2.3. Synthesis of PCM composites

The ternary eutectic, denoted Na_x(Cl, Br, MoO_4), was obtained according to a previously described procedure [27]. In brief, the hydrated eutectic salt mixture was prepared by mixing NaCl, NaBr and $Na_2MoO_4{\cdot}2H_2O$ in a 5:40:55 molar ratio. Before being used NaCl and NaBr were dried for 1 hour at 150 °C.

In a typical synthesis of PCM composites, 50 mg of MCF were mixed with aqueous solution of NaCl, NaBr and Na_2MoO_4) with a concentration of 500 gL^{-1} of salts and then water was removed under vacuum. Depending on the desired eutectic salt content in PCM composite, multiple impregnation steps followed by water evaporation were carried out (Table 1).

Table 1

Experimental obtaining conditions

Sample	Salt eutectic content (% wt.)	Impregnation steps
70%Na_x(Cl,Br,MoO_4)@MCF	70.0	1
80%Na_x(Cl,Br,MoO_4)@MCF	80.0	2
85%Na_x(Cl,Br,MoO_4)@MCF	85.0	3
92.5%Na_x(Cl,Br,MoO_4)@MCF	92.5	6

2.4. Characterization

Wide-angle X-ray diffraction (XRD) were performed using a Rigaku MiniFlex II diffractometer with Cu-Ka radiation (λ = 1.5406 Å). The textural analysis of the samples was performed through nitrogen physisorption at -196 °C, using a Micromeritics ASAP 2020 analyzer. The specific surface area values were calculated using the Brunauer-Emmett-Teller (BET) equation and the total pore volume was estimated from the amount of adsorbed gas at the relative pressure of 0.99. The values on the desorption branches of the isotherms were used to plot the pore size distribution curves using the Barrett Joyner Halenda method. Scanning electron microscopy (SEM) coupled with energy dispersive X-ray spectroscopy (EDX) was carried out using a Tescan Vega 3 LM electron microscope. Thermogravimetric analyses (TG) were performed using a Mettler Toledo TGA/SDTA851e, at a heating rate of 10 °Cmin^{-1}, in closed alumina crucibles with pierced lids and under synthetic air flow. Shape – stability was assessed using a Carl Zeiss Jena high temperature microscope, equipped with a digital optical camera. Samples were heated from 25 °C to 600 °C with a 10 °Cmin^{-1} heating rate. Differential scanning calorimetry (DSC) analyses were carried out on a Mettler Toledo DSC3, at a 10 °Cmin^{-1} heating rate, under 60 mLmin^{-1} nitrogen flow, using pierced lid aluminum crucibles. Thermal reliability was investigated similarly according to our previously reported procedure by carrying out 100 heating cooling cycles using the Mettler Toledo DSC3 equipment.

3. Results and discussion

3.1. Characterization of PCM composites

The porosity of the matrix and its morphology were reported elsewhere [28]. The matrix has an “ink-bottle” mesopore structure, consisting of larger, spherical

cells connected by smaller, cylindrical windows. The matrix has a specific surface area of 463 m^2g^{-1}, total pore volume of 2.35 cm^3g^{-1} and an average pore diameter of 33.8 nm for the spherical cells, while the small cylindrical windows and average pore diameter of 18.8 nm. MCF matrix consists of spherical particles with a diameter of 4 μm.

Scanning electron microscopy coupled with energy dispersive X-ray spectroscopy was used to study the morphology and the distribution of the eutectic components. It results that the morphology of the matrix is preserved after ternary eutectic loading. The composites consist of large aggregates, up to 50 μm, which are composed of micron sized particles of ternary eutectic salt and MCF silica (Figure 1). The elements mapping acquired with the EDX detector indicates that the ternary eutectic and silica particles are mixed with a high degree of homogeneity.

The crystallinity of the samples containing salts was assessed using wide-angle XRD (Fig. 2). The results show that all the composites have similar diffraction patterns to the pristine ternary eutectic mixture, indicating the presence of crystalline salts [27], necessary for thermal energy storage. The wide-angle XRD measurements confirm that the prepared composites samples can serve as PCMs.

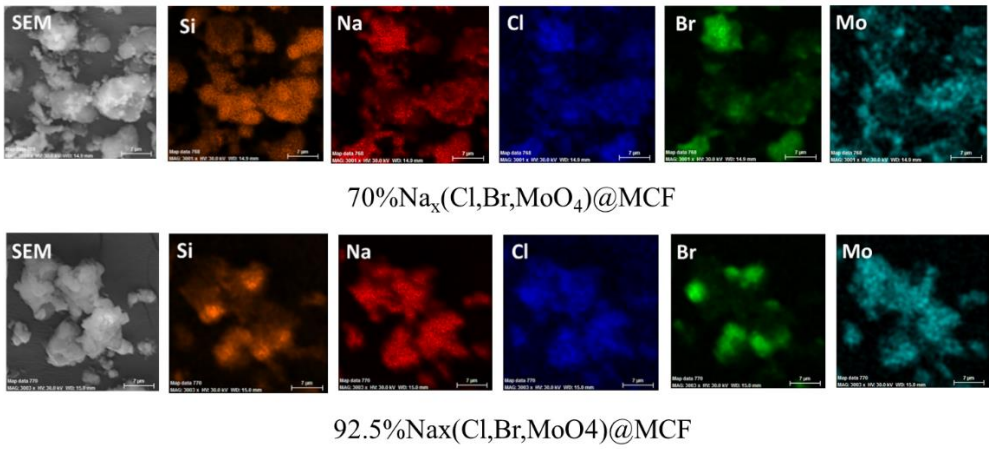

Fig. 1: SEM images and EDX mapping of 70%Na_x(Cl,Br,MoO_4)@MCF and 92.5%Na(Cl,Br,MoO_4)@MCF samples

3.2. Thermal and shape stability

The thermal stability of the PCM composites was assessed by thermogravimetric (TG) analysis (Fig. 3). The ternary eutectic salt undergoes a mass loss of approximately 11.20% when heated from 25 to 150 °C, which can be

attributed to the removal of the crystallization water molecules from $Na_2MoO_4 \cdot 2H_2O$. The observed mass loss is in agreement with the theoretical mass loss value of 11.17%, which was calculated based on the eutectic's composition. A variable water content was noticed. The ternary eutectic salt as well as the composites are stable up to 650 °C, after which significant mass loss is noticed. The mass loss at high temperature could be explained by the decomposition of the molten eutectic salt. It can be concluded that the nanostructured composite samples are thermally stable up to at least 650 °C.

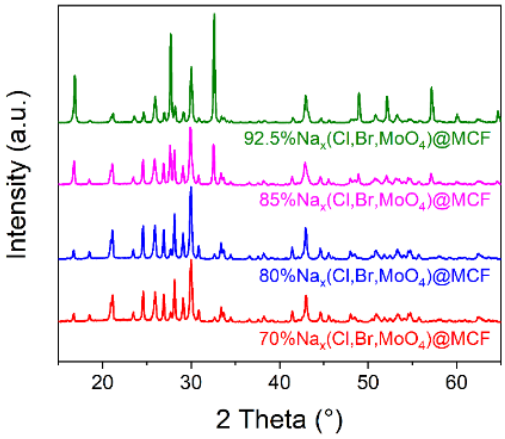

Fig. 2: XRD patterns of the composite samples

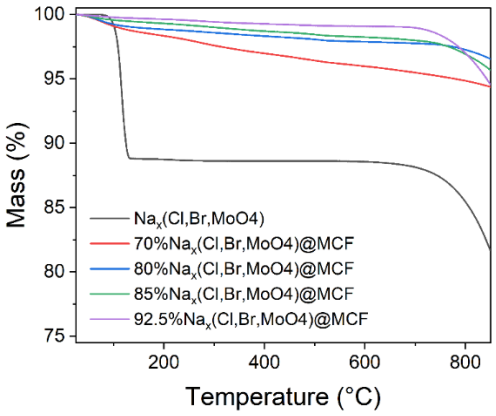

Fig. 3: Thermogravimetric analysis of the ternary eutectic salt and composite samples.

The pristine ternary eutectic and composite samples were analyzed using an optical microscope at high temperature to assess the ability to maintain their macroscopic solid shape when heated above the melting point of the salt. This ability is known as shape – stability and is due to capillary forces that allow the material to retain its shape after the solid – liquid phase transition. The samples were heated from 20 °C to above 550 °C with a heating rate of 10 °Cmin^{-1}. Pictures were taken initially at 20 °C, above 550 °C and at temperatures corresponding to DSC thermal events of the pristine eutectic salt (Fig. 4). The thermal event from 450 ° – 480 °C corresponds to the solid-solid transition in Na_2MoO_4, while the one from 520 – 550 °C to the melting of the ternary eutectic salt (Fig. 5). The initial samples were in the form of powders, which were composed of tiny particles that had a diameter of less than 1 millimeter (Fig. 1). No significant transformations were observed in the case of any sample at 450 – 480 °C. At a temperature of 520 – 550 °C, the pristine eutectic is almost entirely liquefied, and when the temperature is increased beyond the melting point, the mixture goes into a fully liquid state. This transformation is indicated by the formation of a continuous film at 550 °C. On the other hand, all composites maintain their shape when exposed to a temperature that surpasses the melting point of the eutectic mixture. The composites become more compact, causing a reduction in sample volume when heated above the salt melting point. This phenomenon occurs because the composite undergoes densification. Overall, the obtained PCM composites maintain their macroscopic solid shape above the melting point of the eutectic mixture and can be considered as shape-stabilized materials.

3.3. Thermal energy storage properties

The thermal properties of the ternary eutectic and composite materials were assessed by differential scanning calorimetry through heating – cooling cycles. The heat of fusion and melting point values were computed from the 2nd cycle and no humidity correction was applied.

The ternary eutectic mixture presents two thermal events with T_{onset} at 454.5 °C and 522.1 °C, both being endothermic (Fig. 5 A). The event found at lower temperature corresponds to the solid – solid phase transition of Na_2MoO_4, from the eutectic mixture. According to the literature, the salt component undergoes phase transition from cubic to orthorhombic structure in the temperature range of 444 °– 460 °C [29]. The solid-solid phase transition of Na_2MoO_4 was also confirmed in the previous study [27]. Upon heating, the ternary eutectic mixture has a total enthalpy change of 216.2 Jg^{-1} from which 137.3 Jg^{-1} corresponds to the melting of the mixture and the rest to the solid - solid phase transition (Table 2).

During the heating run the PCM composites have at least two endothermic events, corresponding to the solid – solid and solid – liquid transitions. The

additional events most likely represent nanoconfined solid-solid and nanoconfined solid-liquid since a temperature decrease for the events are noticed with respect to the pristine eutectic mixture. The exothermic transitions during cooling of all materials including that of the ternary eutectic indicate that the phase transitions are reversible.

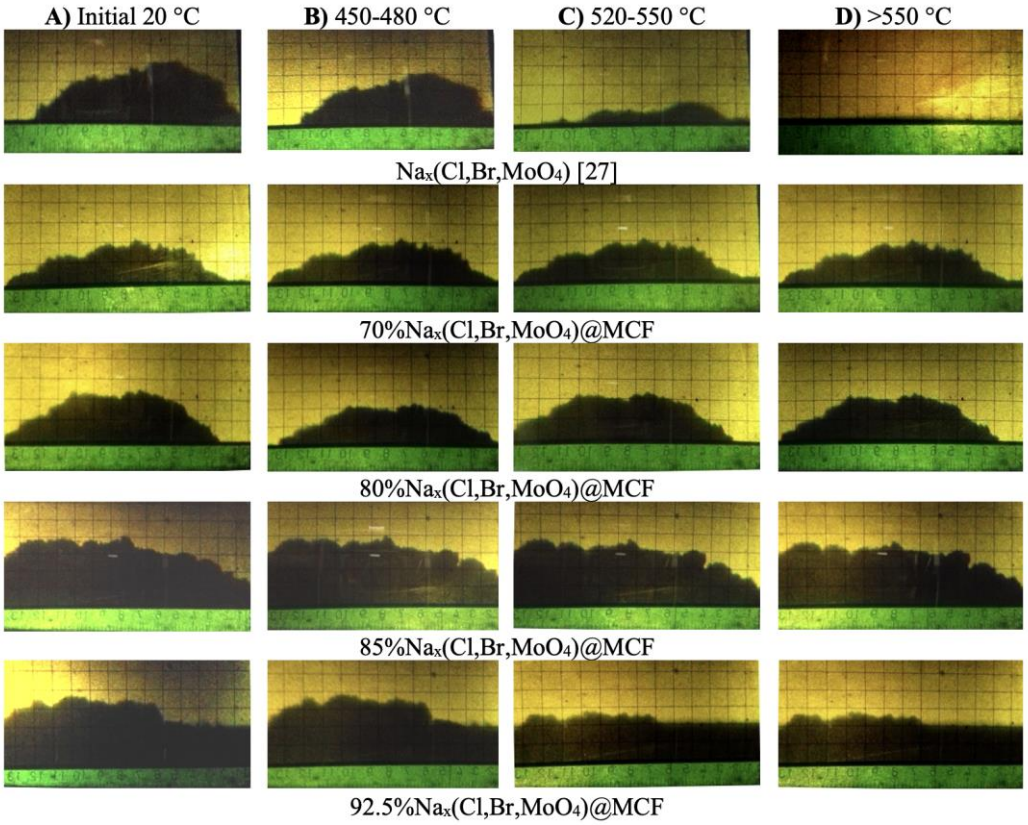

Fig. 4: Pictures recorded on an optical microscope of the samples at the beginning of the heating run, at 20 °C (A), at the solid-solid phase transition of Na_2MoO_4 (B), at the melting point (C) and above the melting point (D).

The sample containing 92.5% eutectic (Fig. 5 E) has a similar behavior to the pristine eutectic salt (Fig. 5 A). For this sample, the solid-liquid transition temperature increased compared to that of the pristine eutectic, indicating a deviation from the eutectic stoichiometry. In the case of the sample with 85% eutectic, for the solid – liquid transition two superimposed events are observed (Fig. 5 D), which can be attributed to the salt particles nanoconfined into the pores of silica matrix and in the interparticle region. In the case of the samples with a higher content of mesoporous silica matrix (Fig. 5 B and C) an additional thermal event

can be noticed that is likely caused by a solid-solid transition of a nanoconfined phase of Na_2MoO_4.

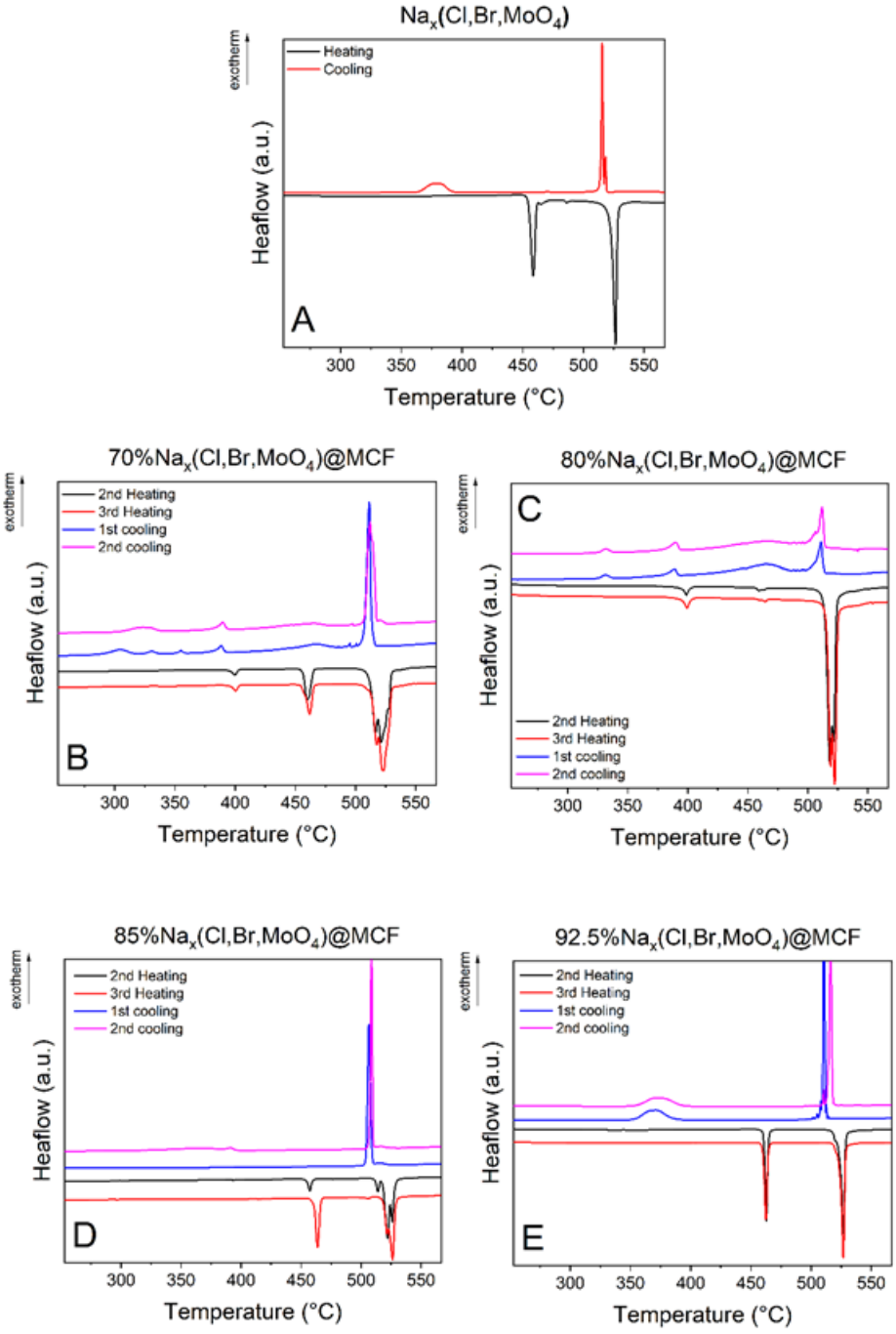

Fig. 5: DSC analyses of the ternary eutectic and composite samples

Table 2

Thermal properties of the ternary eutectic and PCM composites

Sample $Na_x(Cl,Br,MoO_4)$ content in MCF	NC Solid - solid transition (~390 °C)		Solid – solid Transition (~460 °C)		Solid – liquid Transition (~520 °C)		Total ΔH	
	T (°C)	Δ*H* (Jg^{-1})	*T* (°C)	Δ*H* (Jg^{-1})	*T* (°C)	Δ*H* (Jg^{-1})	(Jg^{-1})	(%)
Eutectic mixture **[27]**	-	-	454.5	78.9	522.1	137.3	216.2	100
70%	395.7	3.2	456.2	19.4	514.6	104.2	126.7	58.6
80%	395.8	2.8	456.8	1.3	515.0	96.0	100.1	46.3
85%	-	-	454.6	14.0	518.0	134.4	148.3	68.6
92.5%	-	-	460.6	74.1	523.3	137.3	211.4	97.8

NC - nanoconfined

The thermal reliability of the PCM composite containing 70% eutectic mixture was assessed by performing 100 heating – cooling cycles between 280 ° and 560 °C. The first 6 cycles and afterwards every 5th cycle were recorded. The enthalpy for each thermal event on heating as a function of cycle numbers is shown in Fig. 6.

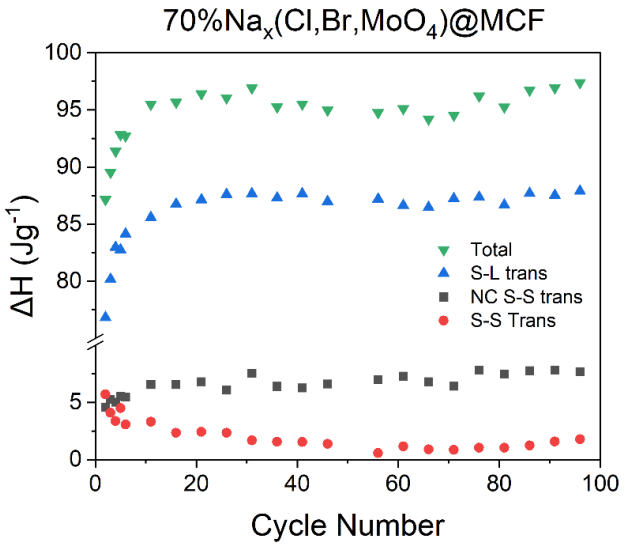

Fig. 6: Thermal reliability of the 70% Na_x(Cl, Br, MoO_4)@MCF sample (S – L trans means solid – liquid transition; NC – nanoconfined phase; S – S solid – solid transition)

The enthalpy corresponding to solid – liquid transition gradually increases in the first 30 cycles, suggesting that fusion takes place between the eutectic mixture

particles. On the other hand, the enthalpy associated with the nanoconfined solid – solid phase of the Na_2MoO_4 eutectic increases, while the enthalpy corresponding to the solid – solid transition decreases, in the first 10 cycles. This behavior suggests that the nanoconfined Na_2MoO_4 phase from the eutectic mixture increases, which could be caused by adsorption of this phase into the mesopores. Overall, the sample has a total heat of fusion ~96 Jg^{-1} at the 35th cycle and retains these values to the end of the experiment suggesting a good thermal reliability.

3.4. The influence of nanoconfinement on phase transitions

The decrease of the transition temperature, which occurs after nanoconfinement can be quantified using the Gibbs-Thomson equation (Eq 1) [30]. This equation is derived from the Clausius – Clapeyron and Kelvin equations, and it arises from the changes in vapor pressure over menisci in small capillaries [31]. The term A in equation 1, which contains all constants, was estimated to be 330.15 nmK for the ternary eutectic melting in a previous study [27]. A value of 488.89 nmK was obtained for the A term in the case of the solid – solid transition of Na_2MoO_4 using the same procedure.

$$T(\infty) - T(r) = \frac{T(\infty)\cdot M\cdot \gamma_{sl}}{\rho\cdot \Delta H_f}\cdot\frac{\alpha}{r}\cos\theta = \frac{A}{r} \quad (1)$$

where $T(\infty)$ and $T(r)$ are the melting temperatures of bulk and nanoconfined phase corresponding to a radius r, respectively, M, ρ and ΔH_f are the molar weight, density and heat of fusion, respectively, γ_{sl} represents the surface tension of the solid – liquid interface, α is a geometric shape parameter and θ is the contact angle, typically assumed 180°; A is a term containing all constants.

The ternary eutectic average diameter computed using the Gibbs-Thomson equation increases from 88 nm for the sample containing 70 % wt. salt to 92 and 162 nm for the materials with 80 % wt. and 85 % wt. salt, respectively (Fig. 7). The ternary particle diameters are higher than the average pore diameter, indicating that the salt is confined in the interparticle space. The 92.5%Na_x(Cl,Br,MoO_4)@MCF sample does not have a melting point depression, suggesting that no interparticle nanoconfinement takes place. The solid-solid transition of Na_2MoO_4 was subjected to a similar treatment. Average diameter value of 16.6 nm was obtained for both composites containing 70% and 80% wt. eutectic, which might indicate that the molybdate is nanoconfined inside the MCF mesopores (Fig. 7).

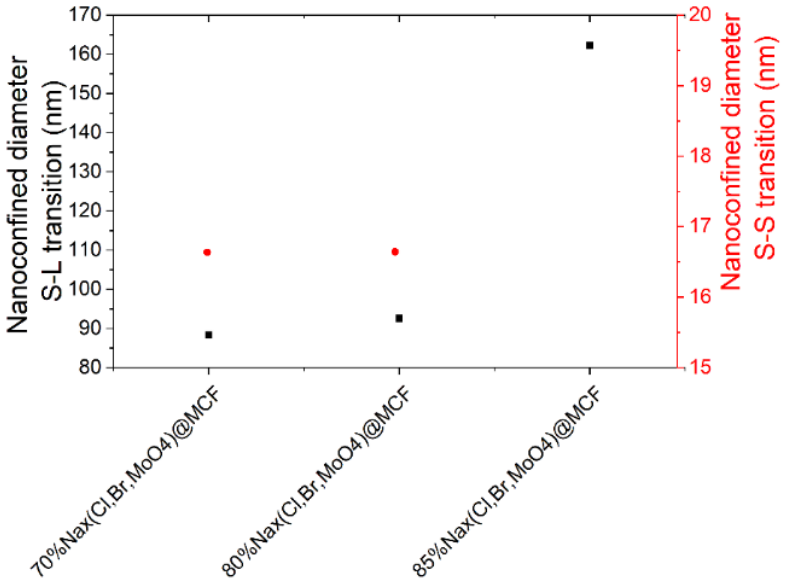

Fig. 7: Average diameters of the ternary salt and Na_2MoO_4 computed using the Gibbs-Thomson equation for the solid – liquid and solid – solid transitions, respectively.

The average diameter values of the ternary salt eutectic were also computed for the 50 heating – cooling cycles performed on the 70%Na_x(Cl, Br, MoO4)@MCF sample (Fig. 8).

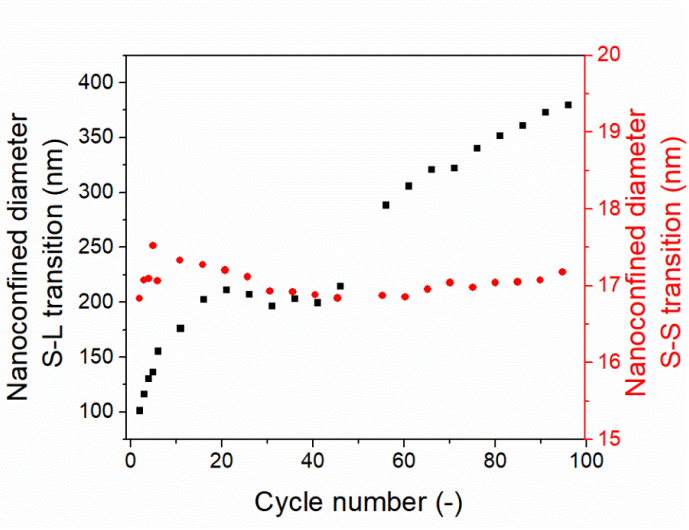

Fig. 8: Variation of nanoconfined average salt diameter over 50 heating - cooling cycles for 70%Na_x(Cl, Br, MoO_4)@MCF sample

The ternary salt diameter increases with each cycle, from 101 nm for the first cycle to 380 nm after 50 cycles. The diameter increase suggests that the ternary salt eutectic particles undergo fusion and sintering, in accordance with the thermal reliability enthalpy data. In contrast to the case of the ternary salt eutectic, the average diameter of the Na_2MoO_4 phase remains relatively constant during the 50 heating – cooling cycles, being in the range of 17 – 18 nm, probably because a significant fraction of sodium molybdate is inside silica mesopores.

4. Conclusions

High temperature shape – stabilized PCMs composed of 5% NaCl, 40% NaBr and 55% Na_2MoO_4 as an active heat storage phase and MCF silica as matrix were studied for thermal energy system in concentrated solar power technology. A previously reported impregnation method for the PCM was optimized in terms of salt content and obtaining procedure. Composites containing 70%, 80%, 85% and 92.5% wt. eutectic salt mixture were obtained.

A good homogeneity of the MCF matrix and the active storage phase was observed through SEM for PMCs. The thermal stability was investigated by TG analysis, which showed that the composites are stable up to 650 °C. For all composite samples was demonstrated the shape – stability at a temperature exceeding the melting point of the ternary eutectic mixture.

During heating run, the ternary eutectic has two thermal events with T_{onset} = 454.5 °C corresponding to a Na_2MoO_4 solid – solid transition and 522.1 °C, the eutectic melting point, both being endothermic. The solid – solid phase transition temperature of Na_2MoO_4 and the melting point of the eutectic mixture in the composite samples were lower which can be explained by nanoconfinement effect. The PCMs with a higher content of MCF (in the range of 20-30%) showed two additional thermal events that can be associated with a nanoconfined solid-solid and nanoconfined solid-liquid phase at lower temperatures than those of the pristine eutectic mixture. The phase transition and melting temperature were estimated using Gibbs – Thompson equation, which correlates the melting point and phase transition temperature decrease with the particle size. The computed particle dimension of the nanoconfined eutectic mixture is higher than the MCF silica pore size suggesting that it is confined in the interparticle region and not in MCF pores. On the other hand, the computed particle size of the nanoconfined Na_2MoO_4 is lower than the pore size of MCF indicating that this phase could be nanoconfined in the pores.

The samples containing 92.5 %wt. and 80 %wt. eutectic mixture have the total ΔH of 211.43 Jg^{-1}, and 148.34 Jg^{-1}, respectively. The sample containing 80 %wt. eutectic salt represents the optimal PCMs, with regards to its shape – stability for TES applications. A slight increase in the total ΔH is noticed in the first 35

heating – cooling cycles, suggesting that fusion takes place between the salt particles. After the 35th cycle, no further significant changes are undergone suggesting that the materials are thermally reliable for energy storage.

In contrast to the previous study, the optimized obtaining method resulted in PCMs with similar shape – stability, energy storage and thermal stability and reliability. In addition, due to the optimized synthesis method, more evidence regarding nanoconfinement effects of Na_2MoO_4 solid – solid phase transition could be observed, and a higher thermal reliability was achieved.

REFERENCES

[1]. *E.W. Law, M. Kay, R.A. Taylor*, Calculating the financial value of a concentrated solar thermal plant operated using direct normal irradiance forecasts, in Solar Energy, **vol. 125**, 2016, pp. 267-281.

[2]. *P. Pardo, A. Deydier, Z. Anxionnaz-Minvielle, S. Rougé, M. Cabassud, P. Cognet*, A review on high temperature thermochemical heat energy storage, in Renewable and Sustainable Energy Reviews, **vol. 32**, 2014, pp. 591-610.

[3]. *A. Calderón, C. Barreneche, A. Palacios, M. Segarra, C. Prieto, A. Rodriguez-Sanchez, A.I. Fernández*, Review of solid particle materials for heat transfer fluid and thermal energy storage in solar thermal power plants, in Energy Storage, **vol. 1**, no. 4, 2019, pp. e63.

[4]. *R.-A. Mitran, S. Ioniţă, D. Lincu, D. Berger, C. Matei,* A Review of Composite Phase Change Materials Based on Porous Silica Nanomaterials for Latent Heat Storage Applications, in Molecules, **vol. 26**, no. 1, 2021, pp. 241.

[5]. *B.D. Iverson, S.T. Broome, A.M. Kruizenga, J.G. Cordaro*, Thermal and mechanical properties of nitrate thermal storage salts in the solid-phase, in Solar Energy, **vol. 86**, no. 10, 2012, pp. 2897-2911.

[6]. *Z. Liu, Z. Yu, T. Yang, D. Qin, S. Li, G. Zhang, F. Haghighat, M.M. Joybari*, A review on macro-encapsulated phase change material for building envelope applications, in Building and Environment, **vol. 144**, 2018, pp. 281-294.

[7]. *H. Qi, T. Zhang, D. Zhang, K. Wang, Y. Wang*, Paraffin/chitosan composite phase change materials fabricated by piercing-solidifying method for thermal energy storage, in AIP Advances, **vol. 10**, no. 3, 2020, pp. 035218.

[8]. *D. Lincu, S. Ioniţă, B. Trică, D.C. Culita, C. Matei, D. Berger, R.-A. Mitran*, Bismuth-mesoporous silica-based phase change materials for thermal energy storage, in Applied Materials Today, **vol. 29**, 2022, pp. 101663.

[9]. *Z. Xiangfa, X. Hanning, F. Jian, Z. Changrui, J. Yonggang*, Pore structure modification of silica matrix infiltrated with paraffin as phase change material, in Chemical Engineering Research and Design, **vol. 88**, no. 8, 2010, pp. 1013-1017.

[10]. *Y. Zhang, S. Zheng, S. Zhu, J. Ma, Z. Sun, M. Farid*, Evaluation of paraffin infiltrated in various porous silica matrices as shape-stabilized phase change materials for thermal energy storage, in Energy Conversion and Management, **vol. 171**, 2018, pp. 361-370.

[11]. *R.A. Mitran, D. Berger, C. Munteanu, C. Matei*, Evaluation of Different Mesoporous Silica Supports for Energy Storage in Shape-Stabilized Phase Change Materials with Dual Thermal Responses, in The Journal of Physical Chemistry C, **vol. 119**, no. 27, 2015, pp. 15177-15184.

[12]. *R.-A. Mitran, D. Berger, C. Matei*, Improving thermal properties of shape-stabilized phase change materials containing lauric acid and mesocellular foam silica by assessing thermodynamic properties of the non-melting layer, in Thermochimica Acta, **vol. 660**, 2018, pp. 70-76.

[13]. *D. Chen, Y. Chen, X. Guo, W. Tao, J. Wang, S. Gao, J. Gao*, Mesoporous silica nanoparticles with wrinkled structure as the matrix of myristic acid for the preparation of a promising new shape-stabilized phase change material via simple method, in RSC Advances, **vol. 8**, no. 60, 2018, pp. 34224-34231.

[14]. J. Gao, W. Tao, D. Chen, X. Guo, Y. Chen, Y. Jiang, High Performance Shape-Stabilized Phase Change Material with Nanoflower-Like Wrinkled Mesoporous Silica Encapsulating Polyethylene Glycol: Preparation and Thermal Properties, in Nanomaterials, **vol. 8**, no. 6, 2018.

[15]. *D. Feng, Y. Feng, P. Li, Y. Zang, C. Wang, X. Zhang*, Modified mesoporous silica filled with PEG as a shape-stabilized phase change materials for improved thermal energy storage performance, in Microporous and Mesoporous Materials, **vol. 292**, 2020, pp. 109756.

[16]. *Y. Wu, T. Wang*, Preparation and characterization of hydrated salts/silica composite as shape-stabilized phase change material via sol–gel process, in Thermochimica Acta, **vol. 591**, 2014, pp. 10-15.

[17]. *Y. Wu, T. Wang*, Enthalpy of solid−liquid phase change confined in porous materials, in Industrial and Engineering Chemistry Research, **vol. 55**, no. 44, 2016, pp. 11536-11541.

[18]. *R.-A. Mitran, S. Petrescu, S. Şomăcescu, O.C. Mocioiu, L. Buhălţeanu, D. Berger, C. Matei*, Nanocomposite phase change materials based on NaCl–CaCl2 and mesoporous silica, in Journal of Thermal Analysis and Calorimetry, **vol. 138**, no. 4, 2019, pp. 2555-2563.

[19]. *T. Qian, J. Li, X. Min, Y. Deng, W. Guan, L. Ning*, Radial-like mesoporous silica sphere: A promising new candidate of supporting material for storage of low-, middle-, and high-temperature heat, in Energy, **vol. 112**, 2016, pp. 1074-1083.

[20]. *A.-M. Brezoiu, M. Deaconu, I. Nicu, E. Vasile, R.-A. Mitran, C. Matei, D. Berger*, Heteroatom modified MCM-41-silica carriers for Lomefloxacin delivery systems, in Microporous and Mesoporous Materials, **vol. 275**, 2019, pp. 214-222.

[21]. *R.-A. Mitran, D. Lincu, L. Buhălţeanu, D. Berger, C. Matei*, Shape-stabilized phase change materials using molten NaNO3 – KNO3 eutectic and mesoporous silica matrices, in Solar Energy Materials and Solar Cells, **vol. 215**, 2020, pp. 110644.

[22]. *M. Deaconu, I. Nicu, R. Tincu, A.-M. Brezoiu, R.-A. Mitran, E. Vasile, C. Matei, D. Berger*, Tailored doxycycline delivery from MCM-41-type silica carriers, in Chemical Papers, **vol. 72**, no. 8, 2018, pp. 1869-1880.

[23]. *S.-H. Wu, C.-Y. Mou, H.-P. Lin*, Synthesis of mesoporous silica nanoparticles, in Chemical Society Reviews, **vol. 42**, no. 9, 2013, pp. 3862-3875.

[24]. *R.-A. Mitran, D.C. Culita, I. Atkinson*, Thermal stability enhancement of mesoporous SBA-15 silica through nanoconfinement of ceria nanoparticles, in Microporous and Mesoporous Materials, **vol. 306**, 2020, pp. 110484.

[25]. *M.M. Kenisarin*, High-temperature phase change materials for thermal energy storage, in Renewable and Sustainable Energy Reviews, **vol. 14**, no. 3, 2010, pp. 955-970.

[26]. *S.E.E. Huseyin Murat Cekirge, Richard Stanley Thorsen*, The CSP (Concentrated Solar Power) Plant with Brayton Cycle: A Third Generation CSP System, in American Journal of Modern Energy, **vol. 6**, no. 1, 2020, pp. 43-50.

[27]. *R.A. Mitran, D. Lincu, S. Ioniţă, M. Deaconu, V.V. Jerca, O.C. Mocioiu, D. Berger, C. Matei*, High temperature shape – Stabilized phase change materials obtained using mesoporous silica and NaCl – NaBr – Na_2MoO_4 salt eutectic, in Solar Energy Materials and Solar Cells, **vol. 218**, 2020, pp. 110760.

[28]. *D. Lincu, S. Ioniţă, O.C. Mocioiu, D. Berger, C. Matei, R.A. Mitran*, Aluminum doping of mesoporous silica as a promising strategy for increasing the energy storage of shape stabilized phase change materials containing molten $NaNO_3$: KNO_3 eutectic mixture, in Journal of Energy Storage, **vol. 49**, 2022, pp. 104188.

[29]. *C.L. Lima, G.D. Saraiva, P.T.C. Freire, M. Maczka, W. Paraguassu, F.F. de Sousa, J. Mendes Filho*, Temperature-induced phase transformations in Na_2WO_4 and Na_2MoO_4 crystals, in Journal of Raman Spectroscopy, **vol. 42**, no. 4, 2011, pp. 799-802.

[30]. *O.V. Petrov, D. Vargas-Florencia, I. Furó*, Surface Melting of Octamethylcyclotetrasiloxane Confined in Controlled Pore Glasses: Curvature Effects Observed by 1H NMR, in The Journal of Physical Chemistry B, **vol. 111**, no. 7, 2007, pp. 1574-1581.

[31]. *K.C. Hugo*, Confinement effects on freezing and melting, in Journal of Physics: Condensed Matter, **vol. 13**, no. 11, 2001, pp. R95.